

Optical Spatial Modulation with DHT-Based OFDM in Visible Light Communication Systems

Yali Cao¹, Xiaotian Zhou¹, Jian Sun¹, Wensheng Zhang¹, and Cheng-Xiang Wang²

¹Shandong Provincial Key Lab of Wireless Communication Technologies,

School of Information Science and Engineering, Shandong University, Jinan, Shandong, 250100, P.R.China.

²Institute of Sensors, Signals and Systems, School of Engineering & Physical Sciences, Heriot-Watt University, Edinburgh, EH14 4AS, UK.
Email: sdu_caoyali@sina.com, xtzhou@sdu.edu.cn, sunjian@sdu.edu.cn, zhangwsh@sdu.edu.cn, cheng-xiang.wang@hw.ac.uk

Abstract—In this paper, a novel orthogonal frequency division multiplexing (OFDM) modulation scheme based on discrete Hartley transform (DHT) combined with optical spatial modulation (OSM) is proposed for visible light communication (VLC) systems. In the proposed scheme, the function of the conventional discrete Fourier transform (DFT) is fulfilled by the DHT and real constellation schemes such as binary phase shift keying (BPSK) and pulse amplitude modulation (PAM) can be used. Hence, real signals are generated and then modulated to two light emitting diodes (LEDs) by employing OSM. The zero-forcing (ZF) scheme and maximum a posteriori (MAP) scheme are employed in the receiver. Simulation results indicate that the proposed scheme can achieve the required performance in terms of bit error rate (BER). The performance of Non-DC-biased OFDM (NDC-OFDM), generalized LED index modulation optical OFDM (GLIM-OFDM), and the proposed scheme is compared. It is shown that the proposed scheme has lower complexity than NDC-OFDM, and shows better BER performance and higher design flexibility than GLIM-OFDM.

Index Terms—VLC, MIMO-OFDM, optical spatial modulation, discrete Hartley transform (DHT), BER

I. INTRODUCTION

Nowadays, there has been looming radio frequency (RF) spectrum crisis as mobile data demands increase rapidly. VLC has drawn significant attention due to its operation in rich license-free bandwidths ranging from 400 THZ to 800 THZ [1]. Illumination and communication can be realized simultaneously in VLC systems and unlike in RF systems, there is no interference from sensitive electronic equipments. Since the information is transmitted by the intensity of light, VLC systems in general have low energy consumption and good security performance. The integration of VLC into the existing lighting infrastructure becomes possible as efficient and cheap LEDs have been widely used in recent years. Furthermore, VLC has potential to offer high speed data rate by employing some sophisticated techniques such as multiple-input multiple-output-OFDM (MIMO-OFDM) and equalization [2].

In VLC systems, LEDs are used as transmitters to convert the electrical signals into optical signals and photodiodes (PDs) are used as receivers to detect the optical signals directly. OFDM is considered as a promising technology for VLC systems because of its high spectral efficiency and robustness to inter-symbol interference (ISI) [3]. However, conventional OFDM signals in RF systems are always com-

plex and bipolar. Intensity modulation with direct detection (IM/DD) schemes are mostly used in VLC systems [4]. IM/DD schemes require signals to be real-valued and unipolar, so the main challenge for IM/DD based VLC systems is the application of OFDM. Hermitian symmetry is employed to generate real signals in OFDM based schemes. Combined with Hermitian symmetry, DC bias is added in DC biased optical OFDM (DCO-OFDM) to generate real unipolar signals [5]. Hermitian symmetry is also employed in asymmetrically clipped optical OFDM (ACO-OFDM) and unipolar OFDM (U-OFDM) [5], [6]. However, the constraint of Hermitian symmetry halves the spectral efficiency.

Spatial modulation (SM) was proposed as an effective MIMO technique used in VLC systems to achieve higher spectral efficiency [7]. LED arrays also transmitted additional information. NDC-OFDM scheme was proposed in [4] to avoid DC bias by transmitting positive and negative signals with two different LEDs. The positive signals were added to the first LED and the second LED transmitted reverse negative signals. However, Hermitian symmetry was still required in NDC-OFDM. Non-Hermitian symmetry OFDM (NHS-OFDM) proposed in [8] transmitted real and image parts of complex signals by different LEDs, while DC bias was required to convert bipolar signals into unipolar. GLIM-OFDM did not require DC bias or Hermitian symmetry but generalized the LED index modulation concept by transmitting complex OFDM signals by separating these signals into their real-imaginary and positive-negative parts [9], that is, at least four transmit units were required in the GLIM-OFDM system.

This paper proposes an OSM with DHT-based OFDM scheme (dubbed as SH-OFDM) inspired by the concepts of DHT [10] and SM. The Fourier processing is replaced by the real processing of Hartley transform, and real constellations such as BPSK and PAM are employed. After performing inverse DHT (IDHT), real signals are generated directly and then added to two different LEDs by introducing the SM concept. The index of LEDs also transmits information as different LEDs are activated. Compared with NDC-OFDM, Hermitian symmetry is removed, and unlike NHS-OFDM, there is no DC bias in SH-OFDM.

The remainder of this paper is organized as follows. Section II presents the system model. Additionally, transmitter of SH-

TABLE I
COMPARISON OF OPTICAL OFDM BASED SCHEMES.

Optical OFDM scheme (N -point)	NDC-OFDM	NHS-OFDM	GLIM-OFDM	SH-OFDM
Constellation scheme	Complex (M -QAM)	Complex (M -QAM)	Complex (M -QAM)	Real (M -PAM)
DC bias	Not required	Required	Not required	Not required
Hermitian symmetry	Required	Not required	Not required	Not required
Spectral efficiency	$\frac{N-2}{2N} \log_2 M$	$\log_2 M$	$\log_2 M$	$\log_2 M$
Minimum required LEDs number	2	2	4	2

OFDM is illustrated in detail, and optical wireless setup is given. In Section III, receiver of SH-OFDM and corresponding estimation are introduced. Simulation results are provided in Section IV. Finally, Section V concludes the paper.

II. SYSTEM MODEL

A. SH-OFDM for VLC

Fig. 1 shows the transmitter of SH-OFDM. The information bit vector e is mapped into M -PAM symbols x_P where M represents the constellation size and $M = 2$ means the real constellation scheme adopted is BPSK. After performing N -point IDHT, the obtained x_H is further processed to parallel-to-serial (P/S) conversion, and real but bipolar signals x_i are obtained with $i = 0, 1, 2, \dots, N - 1$ for each OFDM symbol. Here, N denotes the number of OFDM subcarrier. To generate unipolar signals, polarity splitter is used to separate x_i into positive x_i^+ and x_i^- as

$$x_i^+ = \begin{cases} x_i, & x_i \geq 0 \\ 0, & x_i < 0 \end{cases} \quad x_i^- = \begin{cases} 0, & x_i \geq 0 \\ -x_i, & x_i < 0 \end{cases} \quad (1)$$

where x_i^+ and x_i^- are digital-to-analog (D/A) converted and then modulated to LED1 and LED2, respectively. LEDs only transmit the absolute value of x_i . Only one LED is activated during one time instance, and the index of LEDs represents additional information.

Table I presents the comparisons of NDC-OFDM, NHS-OFDM, GLIM-OFDM, and the proposed SH-OFDM. As shown in Table I, NHS-OFDM, GLIM-OFDM, and SH-OFDM show identical spectral efficiencies and almost double that of NDC-OFDM for given constellation size M . The halved spectral efficiency of NDC-OFDM results from the Hermitian symmetry it adopts. Compared with NDC-OFDM, NHS-OFDM removes Hermitian symmetry at the expense of lower energy efficiency generated by DC bias. Since there is no Hermitian symmetry or DC bias and complex signals are generated directly by inverse DFT (IDFT) in GLIM-OFDM, at least four LEDs are required so as to convert complex signals into real and unipolar signals.

B. Optical Wireless Setup

Consider an indoor VLC system with N_t transmit units and N_r receive units. Let \mathbf{H} denote the $N_r \times N_t$ optical MIMO

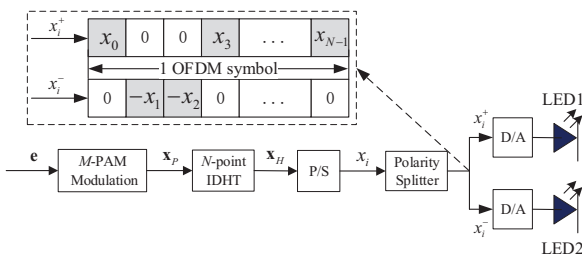


Fig. 1. Transmitter of SH-OFDM for a VLC system.

channel matrix. The element $h_{r,t}$ of \mathbf{H} denotes the channel gain of the optical directed line-of-sight (LOS) link between transmit unit t and receive unit r with $t = 1, 2, \dots, N_t$ and $r = 1, 2, \dots, N_r$. Only the LOS path is taken into consideration in this work as it contains most of the energy and the multi-path components are significantly weak [11]. Hence, $h_{r,t}$ can be calculated as [4], [7]

$$h_{r,t} = \frac{A_r(l+1)}{2\pi d_{r,t}^2} \cos^l(\phi_t) \cos(\psi) T_s(\psi) G_c(\psi) \text{rect}\left(\frac{\psi}{\Psi_c}\right) \quad (2)$$

where $d_{r,t}$ is the distance between transmit unit t and receive unit r , l is the Lambertian order which is defined as $l = -\ln 2 / \ln(\cos \Phi_{1/2})$, $\Phi_{1/2}$ is the transmitter semiangle, A_r is the area of PD. Moreover, ϕ_t and ψ model the radiant angle and the incident angle, respectively. $T_s(\psi)$ is the gain of the optical filter, and $G_c(\psi)$ denotes the concentrator gain. Ψ_c models the concentrator field-of-view (FOV) semiangle, and

$$\text{rect}(x) = \begin{cases} 1, & |x| \leq 1 \\ 0, & |x| > 1. \end{cases} \quad (3)$$

Thus, the optical N_r -dimensional received signals can be obtained as

$$\mathbf{y} = \mathbf{Hx} + \mathbf{w} \quad (4)$$

where \mathbf{x} is the N_r -dimensional transmitted signals and \mathbf{w} is the N_r -dimensional real-valued additive white Gaussian noise (AWGN) vector with mean zero and variance σ_w^2 . The AWGN noise always models shot noise and thermal noise at the optical receiver [9].

Since there is no consensus definition of signal-to-noise ratio (SNR) in VLC systems, the average electrical SNR at each receive unit is considered in this work as each transmit unit is activated with equal probability. The definition is given as [11]

$$\bar{\gamma} = \frac{\bar{P}_r^2}{\sigma_w^2} \quad (5)$$

where \bar{P}_r is the average received optical power at each receive unit. The definition of \bar{P}_r is given as

$$\bar{P}_r = \frac{1}{N_r} \sum_{r=1}^{N_r} P_r \quad (6)$$

and P_r denotes the average received optical power at receive unit r which can be obtained as

$$P_r = \sum_{t=1}^{N_t} h_{r,t} I, \quad (7)$$

where I represents the mean optical intensity being emitted which can be obtained based on the distribution of x_i .

The output vector of N -point IDFT follows Gaussian distribution for large N values if M -QAM symbol is normalized to be unit-energy [9]. In this work, $\hat{\mathbf{x}}_H$, the output vector of N -point IDHT, also follows Gaussian distribution under the same assumption, that is, M -PAM constellation symbol is normalized to be unit-energy and N is large enough. Combined with Parseval's theorem, x_i is conducted to follow standard Gaussian distribution.

III. DETECTION OF SH-OFDM

Fig. 2 shows the SH-OFDM receiver. After analog-to-digital (A/D) conversion, the received signals are fed into SM estimator to reconstruct the bipolar signals \hat{x}_i . After serial-to-parallel (S/P) conversion, $\hat{\mathbf{x}}_H$ is obtained and further applied to perform N -point DHT to get $\hat{\mathbf{x}}_P$. Finally, M -PAM demapping is adopted to recover the information bit vector $\hat{\mathbf{e}}$. In this work, ZF and MAP estimators are employed as SM estimators to detect both the index \tilde{s} and the corresponding signal \tilde{x}_i of the activated LED.

Since there are two LEDs and two PDs in SH-OFDM system, we take $N_t = N_r = 2$ as an example to introduce ZF and MAP estimators as follows. The optical MIMO channel can be written as

$$\mathbf{H} = \begin{bmatrix} h_{1,1} & h_{1,2} \\ h_{2,1} & h_{2,2} \end{bmatrix} \quad (8)$$

and the transmitted signals \mathbf{x} , received signals \mathbf{y} and \mathbf{w} are all 2-dimensional.

A. ZF Estimator

The ZF estimator is used to recover the transmitted information as

$$\tilde{\mathbf{x}} = \mathbf{H}^{-1} \mathbf{y} \quad (9)$$

where \mathbf{H}^{-1} is the inverse matrix of optical MIMO channel \mathbf{H} . Moreover, 2-dimensional $\tilde{\mathbf{x}}$ denotes the estimated transmitted symbols, which can be written as $\tilde{\mathbf{x}} = [x_{i,1} \ x_{i,2}]^T$. To estimate the index \tilde{s} of activated LED, ZF estimator compares the values of the elements in $\tilde{\mathbf{x}}$ as

$$\tilde{s} = \arg \max_s (x_{i,s}), \quad s = 1, 2. \quad (10)$$

Hence, $\tilde{s} = 1$ means LED1 is activated by x_i^+ in the transmitter and the sign of the transmitted signal is positive. On the contrary, LED2 is activated by x_i^- and the sign of the transmitted signal is negative when $\tilde{s} = 2$. As a consequence, the received signal is reconstructed as

$$\hat{x}_i = \begin{cases} \tilde{x}_{i,1}, & \tilde{s} = 1 \\ -\tilde{x}_{i,2}, & \tilde{s} = 2. \end{cases} \quad (11)$$

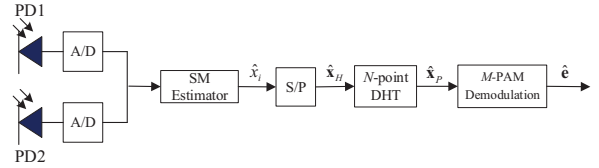


Fig. 2. Receiver of SH-OFDM for a VLC system.

B. MAP Estimator

Note that $x_i \sim N(0, 1)$ and $\bar{x}_i = |x_i|$ follows folded Gaussian distribution with

$$p_{\bar{x}_i}(t) = \frac{\sqrt{2}}{\sqrt{\pi}} e^{-\frac{t^2}{2}} u(t) \quad (12)$$

where $u(t)$ means unit step function. The prior information of \bar{x}_i can be taken into consideration in MAP estimator [9]. The optical MIMO channel \mathbf{H} shown in (8) can be defined as $\mathbf{H} = [\mathbf{h}_1 \ \mathbf{h}_2]$, where \mathbf{h}_1 and \mathbf{h}_2 mean the column vectors. Since there is only one polarity for x_i during one time instance, the optical received signals vector \mathbf{y} given in (4) can be rewritten as $\mathbf{y} = \mathbf{h}_s \bar{x}_i + \mathbf{w}$ with $s \in (1, 2)$. MAP estimator selects the index of the activated LED and corresponding signal as

$$\tilde{x}_{i,s} = \arg \max_{\bar{x}_i} (p(\bar{x}_i|\mathbf{y})) \quad (13)$$

where $p(\bar{x}_i|\mathbf{y})$ represents the probability density function of \bar{x}_i conditioned on \mathbf{y} . Based on Bayes' rule, (13) can be written as

$$\tilde{x}_{i,s} = \arg \max_{\bar{x}_i} (p(\mathbf{y}|\bar{x}_i)p(\bar{x}_i)). \quad (14)$$

Given \bar{x}_k and s , the conditional distribution of \mathbf{y} is $N(\mathbf{h}_s \bar{x}_i, \sigma_w^2)$ and we have

$$\begin{aligned} (\tilde{x}_i, \tilde{s}) &= \arg \max_{\bar{x}_i, s} e^{-[\sigma_w^2 \bar{x}_i^2 + \|\mathbf{y} - \mathbf{h}_s \bar{x}_i\|^2]} \\ &= \arg \min_{\bar{x}_i, s} [\|\mathbf{y} - \mathbf{h}_s \bar{x}_i\|^2 + \sigma_w^2 \bar{x}_i^2]. \end{aligned} \quad (15)$$

Eventually, the received signal \hat{x}_i can be retrieved as

$$\hat{x}_i = \begin{cases} \tilde{x}_i, & \tilde{s} = 1 \\ -\tilde{x}_i, & \tilde{s} = 2. \end{cases} \quad (16)$$

IV. SIMULATION RESULTS

Table II shows the main simulation parameters. We consider a typical room with size of $4 \text{ m} \times 4 \text{ m} \times 3 \text{ m}$ where the LEDs are placed at a height of 0.5 m below the ceiling and the PDs are located at a height of 1 m. LEDs are straight down to the floor and PDs are straight up to the ceiling. Lambertian order, gain of the optical filter, and concentrator gain are all set as 1 for simplicity. A 2×2 MIMO channel and a 4×4 MIMO channel are both considered in the simulations where d_{Rx} was always set as 0.1 m. Line of two LEDs and that of two PDs are aligned parallel in the 2×2 MIMO channel, while four LEDs and four PDs are aligned in square with 2×2 arrays in the 4×4 MIMO channel.

TABLE II
SIMULATION PARAMETERS.

Parameter	Value
Room size, R	$4 \text{ m} \times 4 \text{ m} \times 3 \text{ m}$
DHT and DFT size, N	128
Lambertian order, l	1
Gain of the optical filter, $T_s(\psi)$	1
Concentrator gain, $G_c(\psi)$	1
Reflective index, n	1.5
Half intensity viewing angle, $\Phi_{1/2}$	15°
Receiver FOV semiangle, Φ_c	15°
Physical area of detector, A_r	1 cm^2
Receiver distance, d_{Rx}	0.1 m

A. SH-OFDM vs. NDC-OFDM

First, we analyze the BER performance of the proposed scheme and compare it with that of NDC-OFDM in a 2×2 MIMO channel where two LEDs and two PDs were employed. Let d_{Tx} and d_{Rx} denote the distance between every adjacent two LEDs and PDs, respectively. The positive signals are added to the first LED while the second LED transmits reverse negative signals. Here, d_{Tx} was set as 0.4 m or 0.6 m.

As seen from Fig. 3, MAP estimator exhibits better BER performance than ZF estimator with the same constellation size especially in the channel with higher SNR. Based on (4) and (9), we can get

$$\begin{aligned}\tilde{\mathbf{x}} &= \mathbf{H}^{-1}\mathbf{y} \\ &= \mathbf{x} + \mathbf{H}^{-1}\mathbf{w}.\end{aligned}\quad (17)$$

ZF estimator enhances the power of noise by $\mathbf{H}^{-1}\mathbf{w}$ in spite of its simplicity. MAP estimator considers a priori information for \mathbf{x} to guarantee better BER performance. However, MAP estimator has higher computing complexity than ZF estimator due to its vast searching space. As the value of d_{Tx} increases, the VLC system exhibits better BER performance as the interferences of LEDs become weaker. MAP estimator exhibits obvious superior BER performance with decreasing distance of LEDs.

It is shown in Fig. 4 that with the same data rate and similar hardware configurations, SH-OFDM shows comparable BER performance with NDC-OFDM. However, the constellation size of SH-OFDM is lower than that NDC-OFDM with a relationship of $M_H = \sqrt{M_N}$ where M_H and M_N denote constellation size of SH-OFDM and NDC-OFDM, respectively. Compared with NDC-OFDM, SH-OFDM provides lower complexity by removing Hermitian symmetry. Furthermore, there is no complex operation and DHT is self-inverse in SH-OFDM.

B. P-SH-OFDM vs. GLIM-OFDM

There are 4 transmit units and 4 receive units in the 4×4 MIMO optical channel of GLIM-OFDM system, while SH-OFDM systems employ only 2 transmit units and 2 receive units. To compare the BER performance of this two schemes

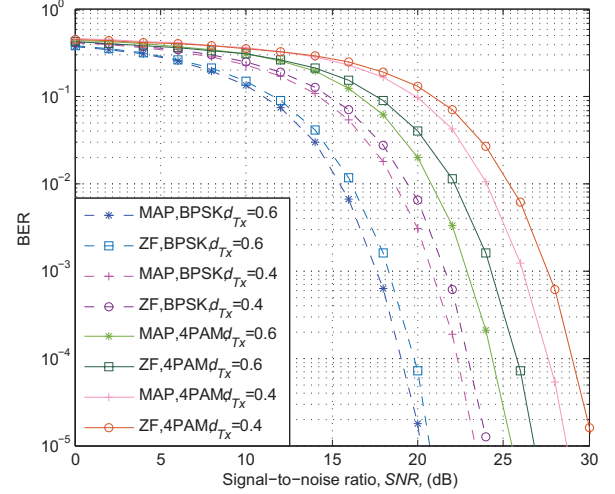


Fig. 3. BER performance of SH-OFDM in a 2×2 MIMO channel.

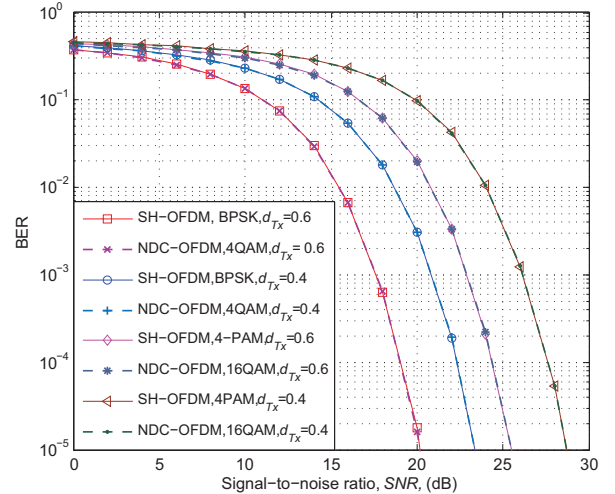


Fig. 4. BER performance comparison of SH-OFDM and NDC-OFDM.

fairly, we consider two-parallel SH-OFDM (P-SH-OFDM) for $N_t = N_r = 4$ with the 4×4 MIMO optical channel as shown in Fig. 5. The first information stream is modulated to LED1 and LED3 with LED1 transmitting positive value and LED3 transmitting reverse negative value. Similarly, the second information stream is modulated to LED2 and LED4. M_G and M_H represent the constellation size of GLIM-OFDM and P-SH-OFDM, respectively. Furthermore, $\sqrt{M_G} = M_H$ in the simulation to ensure the same date rates. To maintain the fairness of the transmitted symbols, we set the energy of M_H -PAM symbols in P-SH-OFDM to be half of that of M_G -PAM symbols in GLIM-OFDM. Here, d_{Tx} was set to be 0.4 m or 0.5 m.

Fig. 6 shows the BER performance comparison of GLIM-OFDM and P-SH-OFDM with MAP estimator. P-SH-OFDM shows better BER performance than GLIM-OFDM under the same data rates with a relationship of $M_H = \sqrt{M_G}$.

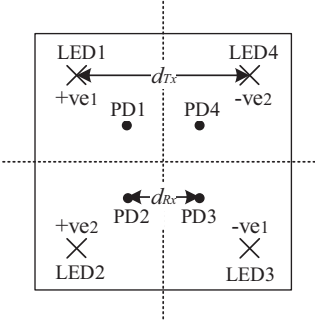


Fig. 5. Placement of LEDs and signal mapping to LEDs in a 4×4 MIMO channel.

Additionally, P-SH-OFDM shows higher design flexibility

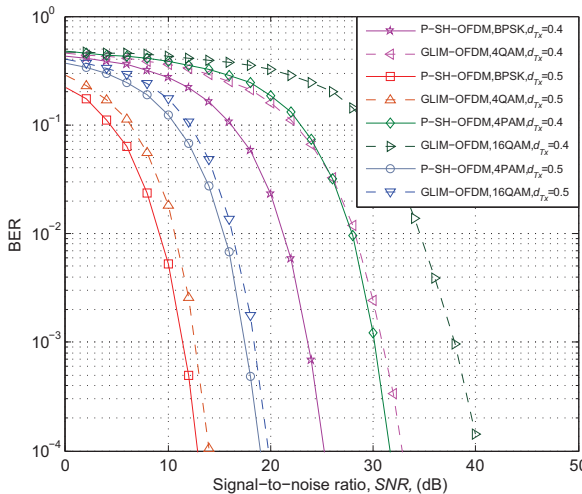


Fig. 6. BER performance comparison of P-SH-OFDM and GLIM-OFDM.

for target data rate since the information data is split into two streams. For example, for a target data rate of 4 bits/s/Hz, GLIM-OFDM employs 16-QAM, that is, $M_G = 16$. However, P-SH-OFDM can employ $M_{H_1} = 2, M_{H_2} = 8$ or $M_{H_1} = 4, M_{H_2} = 4$ where M_{H_1} and M_{H_2} represent the constellation size of PAM in two data streams of P-SH-OFDM, respectively. Hence, simulation results show that P-SH-OFDM outperforms GLIM-OFDM in terms of BER performance and design flexibility.

V. CONCLUSIONS

A novel SH-OFDM scheme has been proposed in this paper. In the proposed scheme, the real processing of Hartley transform replaces the Fourier processing. The direct and inverse transforms are equal in Hartley transform and fast algorithm can also be applied in DHT. The real constellation schemes such as BPSK and PAM have been employed to generate real OFDM symbols directly without complex operation, which may generate advantages since only real signals can be transmitted in optical channels. There is no

Hermitian symmetry or DC bias. Instead, SM has been introduced with Hartley transform to generate unipolar signals. Simulation results have shown that MAP estimator has better BER performance than ZF estimator in the proposed SH-OFDM system. BER performance of GLIM-OFDM, NDC-OFDM, and the proposed SH-OFDM has been compared. Simulation results have shown that NDC-OFDM and SH-OFDM have comparable BER performance, but SH-OFDM has lower size constellation and complexity. It has also been verified that P-SH-OFDM shows superior BER performance and design flexibility than GLIM-OFDM.

ACKNOWLEDGMENT

The authors greatly acknowledge the support from Natural Science Foundation of China (No. 61371110, 61401254), Fundamental Research Funds of Shandong University (No. 2017JC029, 2017JC002), Key R&D Program of Shandong Province (No. 2016GGX101014), Science and Technology Project of Guangzhou (No. 201704030105), EPSRC TOUCAN project (No. EP/L020009/1), and EU H2020 RISE TESTBED project (No. 734325).

REFERENCES

- [1] D. Karunatilaka, F. Zafar, V. Kalavally, and R. Parthiban, "LED based indoor visible light communications: State of the art," *IEEE Commun. Surveys Tuts*, vol. 17, no. 3, pp. 1649–1678, 3rd Quart. 2015.
- [2] P. Pathak, X. Feng, P. Hu, and P. Mohapatra, "Visible light communication, networking and sensing: A survey, potential and challenges," *IEEE Commun. Surveys Tuts*, vol. 17, no. 4, pp. 2047–2077, 4th Quart. 2015.
- [3] F. Barrami, Y. Le Guennec, E. Novakov, and P. Busson, "An optical power efficient asymmetrically companded DCO-OFDM for IM/DD systems," in *Proc. WOCC'14*, Newark, USA, May. 2014, pp. 1–6.
- [4] Y. Li, D. Tsonev, and H. Haas, "Non-DC-biased OFDM with optical spatial modulation," in *Proc. PIMRC'13*, London, UK, Sept. 2013, pp. 486–490.
- [5] S. D. Dissanayake and J. Armstrong, "Comparison of ACO-OFDM, DCO-OFDM and ADO-OFDM in IM/DD systems," *J. Lightw. Technol.*, vol. 31, no. 7, pp. 1063–1072, Apr. 2013.
- [6] D. Tsonev, S. Sinanovic, and H. Haas, "Novel unipolar orthogonal frequency division multiplexing (U-OFDM) for optical wireless," in *Proc. VTC'12-Spring*, Yokohama, Japan, May. 2012, pp. 1–5.
- [7] T. Fath, J. Klaue, and H. Haas, "Coded spatial modulation applied to optical wireless communications in indoor environments," in *Proc. IEEE WCNC'12*, Paris, France, Apr. 2012, pp. 1000–1004.
- [8] W. D. Zhong, C. Chen, and D. Wu, "Non-Hermitian symmetry OFDM for indoor space division multiplexing visible light communications," in *Proc. ICTON'16*, Trento, Italy, Aug. 2016, pp. 1–4.
- [9] E. Başar, E. Panayirci, M. Uysal, and H. Haas, "Generalized LED index modulation optical OFDM for MIMO visible light communications systems," in *Proc. ICC'16*, Kuala Lumpur, Malaysia, May. 2016, pp. 1–5.
- [10] M. S. Morelo, R. Muoz, and G. Junyent, "Novel power efficient optical OFDM based on Hartley transform for intensity-modulated direct-detection systems," *J. Lightw. Technol.*, vol. 28, no. 5, pp. 798–805, Mar. 2010.
- [11] R. Mesleh, H. Elgala, and H. Haas, "Optical spatial modulation," *IEEE/OSA J. Opt. Commun. Netw.*, vol. 3, no. 3, pp. 234–244, Mar. 2011.
- [12] X. Zhou, X. Cheng, and L. Yang, "Quadrature index modulated OFDM for vehicular communications," in *Proc. ICNC'16*, Kauai, USA, Feb. 2016, pp. 1–5.